Magnetic field evolution in Bok globules

Sebastian Wolf

California Institute of Technology, 1201 East California Blvd, Mail code 105-24, Pasadena, CA 91125, USA; swolf@astro.caltech.edu

R. Launhardt and Th. Henning

Max-Planck-Institut für Astronomie, Königstuhl 17, D-69117 Heidelberg, Germany; rl@mpia-hd.mpg.de, henning@mpia-hd.mpg.de

ABSTRACT

Using the Submillimeter Common-User Bolometer Array (SCUBA) at the James Clerk Maxwell Telescope (JCMT), we obtained submillimeter polarization maps of the Bok globules B 335, CB 230, and CB 244 at 850 μ m. We find strongly aligned polarization vectors in the case of B 335 and CB 230, indicating a strong coupling of the magnetic field to the dust grains. Based on the distribution of the orientation and strength of the linear polarization we derive the magnetic field strengths in the envelopes of the globules: $134\mu G$ (B 335), $218\mu G$ (CB 230), and 257μ G (CB 244). In agreement with previous submillimeter polarization measurements of Bok globules we find polarization degrees of several percent decreasing towards the centers of the cores. Furthermore, we compare the magnetic field topology with the spatial structure of the globules, in particular with the orientation of the outflows and the orientation of the nonspherical globule cores. In case of the globules B 335 and CB 230, the outflows are oriented almost perpendicular to the symmetry axis of the globule cores. The magnetic field, however, is aligned with the symmetry axis of the prolate cores in the case of the Bok globules B 335 and CB 230, while it is slightly aligned with the outflow axis in the case of the Bok globules CB 26 and CB 54. We discuss the possibility that the different orientations of the magnetic field relative to the outflow directions reflect different evolutionary stages of the single globules.

Subject headings: Magnetic fields — Polarization — ISM: individual objects: B 335, CB 230, CB 244 — ISM: magnetic fields — Submillimeter

1. Introduction

Bok globules are excellent objects to study the earliest processes of star formation: They are small in diameter (0.1–2 pc), simply structured, and are relatively isolated molecular clouds (Clemens et al. 1991) with masses of 2–100 $M_{\rm sun}$ (Bok 1977, Leung 1985). Low-mass star formation was found to be a common phenomenon in Bok globules: Many globules have bipolar molecular outflows (e.g., Yun & Clemens 1994a) and infrared colors and submillimeter properties that are consistent with Class 0 protostars or embedded Class I sources Yun & Clemens 1994b, Launhardt & Henning 1997 (hereafter LH97); Henning & Launhardt 1998).

To study one of the key parameters of the star formation process – namely the magnetic field – submillimeter polarization measurements represent a powerful technique. Assuming emission by aligned nonspherical grains as the dominating polarization mechanism, where the magnetic field plays a role in the alignment process, magnetic field strengths and structures can be derived from the submillimeter polarization pattern. In the case of Bok globules this has been demonstrated for the first time by Henning et al. (2001; hereafter Paper I). Based on comprehensive preparatory studies such as submillimeter continuum and CS line surveys (LH97; Henning & Launhardt 1998; Launhardt et al. 1997; 1998; in prep.), polarization maps of three Bok globule cores (CB 26, CB 54, and CG 30) had been obtained with SCUBA at $850\,\mu\text{m}$. It was found that the magnetic field strengths derived from polarization patterns are well above those of the interstellar medium (Myers et al. 1995), but are similar to those found in other molecular cloud cores and protostellar envelopes (Bhatt & Jain 1992; Levin et al. 2001; Davis et al. 2000; Glenn, Walker & Young 1999; Itoh et al. 1999; Minchin & Murray 1994; Chrysostomou et al. 1994; Crutcher 1999). The polarization pattern itself revealed striking similarities between the different globules: The degree of polarization amounts to several percent and decreases towards the centers of the dense cores.

Here, we present and discuss new polarization measurements at 850 μ m of protostellar cores in three other nearby Bok globules: B 335 (CB 199), CB 230, and CB 244. As for the previously observed Bok globules, it was our aim to prove basic correlations between the structure and strength of the magnetic field and the dust density distribution which have been investigated theoretically, e.g., by Padoan et al. 2001, Heitsch et al. 2001, Fiege & Pudritz (2000a,c), and Basu & Mouschovias (1995). Combining intensity and polarization maps, the dust density distribution and the magnetic field structure can be found. Due to this enlargement of the sample of spatially resolved polarization maps of Bok globules, the observations were aimed to contribute to the solution of the following problems:

1. Are there systematic differences in the structure and strength of the magnetic field in

the envelopes around low-mass YSOs of different evolutionary stages?

2. Do we see evidence that the magnetic field dominates the structure of globules At which stage of the evolution does the gas decouple from the magnetic fields?

In §2 we compile the main results of previous investigations of our sources. In §3 we give a brief overview about the performed observations and the subsequent data reduction procedure. The polarization maps are presented in §4.1; magnetic field strengths are derived in §4.2, followed by a discussion on the relation between the polarization degree and the intensity in §4.3. Finally, we investigate the correlation between the magnetic field structure and morphological features of the individual globules in §4.4.

2. Source description

In Paper I we investigated submillimeter polarization maps of the Bok globules CB 26, CB 54, and CG 30. In this paper we present new polarization measurements of the Bok globules B 335, (CB 199), CB 230, and CB 244. These six globule cores are the strongest millimeter continuum sources from surveys by LH97 and Henning & Launhardt (1998) surveys accessible with the JCMT/SCUBA. They are the best-studied star-forming Bok-globules.

B 335 (CB 199), an isolated, nearly spherical Bok globule at a distance of ~250 pc (Tomita, Saito, & Ohtani 1979; Frerking, Langer, & Wilson 1987). It accommodates one of the best-studied low-mass protostellar cores (see, e.g., Myers et al. 2000). The deeply embedded Class 0 protostar of $L_{\rm bol} \sim 3 \, {\rm L}_{\odot}$ drives a collimated bipolar outflow with a dynamical age of ~ $3 \times 10^4 \, {\rm yr}$ (Keene et al. 1983; Hirano et al. 1988; Cabrit, Goldsmith, & Snell 1988; Chandler et al. 1990, Chandler & Sargent 1993). The dense core in B 335 is generally recognized as the best protostellar collapse candidate and the emission from different molecular lines has been successfully modeled in terms of an inside-out collapse (Shu 1977) with infall age ~ $10^5 \, {\rm yr}$ and a current protostar mass of ~ $0.4 \, {\rm M}_{\odot}$ (Zhou et al. 1993; Choi et al. 1995). Recent molecular line observations, made with higher angular resolution, show possible discrepancies with the predictions of inside-out collapse (Wilner et al. 2000). From our SCUBA maps, we derive a total envelope mass of ~ $4 \, {\rm M}_{\odot}$ within a radius of $1.5 \times 10^4 \, {\rm AU}$ (Launhardt et al. in prep.). The small C¹⁸O line widths, observed by Frerking et al. (1987), imply a turbulent velocity dispersion of only $0.14 \pm 0.02 \, {\rm km \, s^{-1}}$ in the dense core.

CB230 (L 1177) is a small, bright-rimmed Bok globule associated with the Cepheus Flare molecular cloud complex. While in earlier papers we suggested a distance of 450 pc (LH97), Kun (1998) pointed out that L 1177 is more likely associated with an absorbing sheet at 300 pc. We therefore use a distance of $400\pm100 \text{ pc}$. The globule contains a binary protostellar

core with 10" separation (east-west) with signatures of mass infall which is associated with a double NIR reflection nebula. Both protostars are associated with a NIR reflection nebula and they drive separate aligned molecular outflows, but only the western one is associated with a massive accretion disk (Launhardt et al. 1998; Launhardt 2001). The total mass and luminosity of the protostellar double core, which is unresolved in our SCUBA maps, are $\sim 7 \,\mathrm{M}_{\odot}$ within a radius of $2 \times 10^4 \,\mathrm{AU}$ and $\sim 10 \,\mathrm{L}_{\odot}$, respectively (Launhardt 2001; Launhardt et al. in prep.). The dynamical age of the collimated large-scale outflow is $\sim 2 \times 10^4 \,\mathrm{yr}$ (Yun & Clemens 1994). From the observed C¹⁸O line width of $0.7\pm0.1 \,\mathrm{km \, s^{-1}}$ (Wang et al. 1995; Launhardt 1996) we calculate an upper limit for the turbulent velocity dispersion of $0.29 \pm 0.04 \,\mathrm{km \, s^{-1}}$.

CB 244 (L 1262) is an isolated Bok globule located at a distance of 180 pc and probably associated with the Lindblad ring (LH97; Kun 1998). It contains two dense cores separated by ~ 90". The more prominent south-eastern core, which we observed here, contains a Class 0 protostar with signatures of mass infall. It is associated with a bipolar molecular outflow with a dynamical age of ~ 10⁴ yr (Yun & Clemens 1994; Wang et al. 1995; Launhardt 1996; LH97; Launhardt et al. 1997). The total mass and bolometric luminosity of this protostellar core are ~ 2 M_{\odot} within a radius of 1.8 × 10⁴ AU and ~ 1.5 L_{\odot}, respectively (Wang et al. 1995; Launhardt et al. in prep.). The C¹⁸O line width and turbulent velocity dispersion are the same as for CB 230, i.e., $\sigma_{turb} \sim 0.29 \,\mathrm{km \, s^{-1}}$.

3. Observations and Data reduction

The observations were performed at the 15-m JCMT on Mauna Kea (Hawaii) between September 10 and 14, 2001. The effective beam size (HPBW) at 850μ m is ~ 14.4" at 850μ m. Polarimetry was conducted using SCUBA (Holland et al. 1999) and its polarimeter, SCU-POL with the 350-850 μ m achromatic half-waveplate. For a detailed description of the polarimeter hardware we refer to Murray et al. (1997) and Greaves et al. (2000).

Since our targets have a protostellar core/disk-envelope structure with envelope sizes smaller than 2', we used the imaging mode of SCUBA. Fully sampled 16-point jiggle maps have been obtained for each object, whereby each jiggle map was repeated 16 times with the wave plate turned by 22.5° between the individual maps. This mode allows simultaneous imaging polarimetry with a 2.3 arcminute field of view in the long (750/850 μ m) and short (350/450 μ m) wavelength bands. However, only 850 μ m data are presented in this paper because the signal-to-noise ratio was too low for the 450 μ m polarimetry data.

The data reduction package SURF (SCUBA User Reduction Facility; see Jenness &

Source name ^(a)	Other names ^{(a)}	IRAS source	R.A. (B1950) [h m s]	Dec. (B1950) [° ′ ″]	Dist. [pc]
B 335	CB 199	_	$19 \ 34 \ 35.1^{\rm b}$	$+ 07 27 20^{b}$	$250^{\rm d}$
CB 230	L1177	21169 + 6804	$21 \ 16 \ 53.7^{\rm c}$	$+ 68 04 55^{\circ}$	400
CB244 (SE core)	L1262	23238 + 7401	$23 \ 23 \ 48.5^{c}$	$+ 74 \ 01 \ 08^{c}$	180^{e}

Table 1. Coordinates and distances of the observed globules.

^(a)B: Barnard 1927; L: Lynds 1962; CB: Clemens & Barvainis 1988.

^(b)Coordinates of the submillimeter peak (Huard et al. 1999).

^(c)Coordinates of the 1.3 mm peak (Launhardt et al. in prep.).

 $^{(d)}$ Tomita et al. 1979.

^(e)LH97 (for CB 230 see source description).

 I_{450}^{peak} I_{850}^{peak} F_{450} F_{850} Object $[Jy/\Omega_b]^{(a)} [Jy/\Omega_b]^{(a)}$ [Jy] [Jy] B 335 (CB 199) 3.71.15____ ____ $\operatorname{CB}230$ 16.553.86 2.90.92CB 244 (SE core) 9.11.81.690.49

Table 2. Total and peak fluxes of the observed globules (from Launhardt et al. in prep.).

 $^{(a)} \text{Effective beam sizes}$ (HPBW) $\Omega_{\rm b}$ derived from calibrator maps are 8.5" at 450 $\mu \rm m$ and 14.4" at 850 $\mu \rm m.$

Lightfoot 1998) was used for flat-fielding, extinction correction, sky-noise removal (see Jenness et al. 1998), and instrumental polarization correction. The Stokes parameters I, Q, and U were computed for each set of the 16 maps using the POLPACK data reduction package (Berry & Gledhill 1999) by averaging maps taken at the same wave plate orientation followed by fitting a sine wave to each image pixel. This set of Stokes parameters was then averaged and binned (over a 9" region) before calculating the average linear polarization degree P_1 and position angle γ for each pixel.

Since the chop throw was 120", the very outer regions in the jiggle maps (which are also undersampled) may suffer from chopping into the outermost envelope regions and into extended low-level emission from the tenuous outer regions of the globules. We therefore restrict the polarization analysis to the inner region with a radius of 60" of the maps and do not use the outer ~ 20 ". Based on the 1.2 mm continuum maps obtained by Launhardt et al. (in prep.), we chose arbitrarily a chop throw (azimuthal direction) for B 335 and CB 230, while CB 244 was observed chopping almost perpendicular to the axis defined by the main and the secondary component, in order to avoid the secondary component (see Fig. 1 for illustration).

We restrict the polarization analysis to regions in which the total flux density is higher than 5 times the rms in the maps (measured outside the central sources). Pixels in which the scatter of the total flux density measurements between different jiggle cycles was larger than 20% of the average value were also excluded. Furthermore, polarization vectors with $P_{\rm I}/\sigma(P_{\rm I}) > 3$, where $\sigma(P_{\rm I})$ is the standard deviation of the polarization degree, have been excluded. We found that our selection criteria, which are based on signal-to-noise ratios, result in polarization maps that agree well with those obtained with the default restrictions of ORACDR/POLPACK which use absolute thresholds ($0.1\% < P_{\rm I} < 15\%$ and $\sigma_{\gamma} < 10^{\circ}$).

4. Results

4.1. Polarization maps

Polarized thermal emission by aligned non-spherical grains is the main source of polarized submillimeter radiation in Bok globules (see, e.g., Weintraub et al. 2000, Greaves et al. 1999). The polarization maps of the Bok globules B 335, CB 230, and CB 244 at 850 μ m are shown in Fig. 1. In Figure 2 we plot the polarization histogram for each globule. The degree of linear polarization reaches values up to 14%, whereby the distributions $N(P_1)$ is strongly influenced by statistical noise due to the small number of data points. The mean percentage polarization degrees for B 335, CB 230, and CB 240 are 6.2%, 7.8%,



Fig. 1.— 850 μ m SCUBA maps of B 335 (top), CB 230 (middle), CB 244 (bottom) and with polarization vectors superimposed. The corresponding right ascension and declination of the (0,0) coordinate are given in Tab. 1. The length of the vectors is proportional to the degree of polarization, and the direction gives the position angle. The data are binned over 9". Only vectors for which the 850 μ m flux exceeds 5 times the standard deviation and $P_1/\sigma(P_1) > 3$ are plotted. The contour lines mark the levels of 20%, 40%, 60%, and 80% of the maximum intensity. In case of CB 244, the time-dependent chopping direction during the observation is symbolized in the upper left edge.

Please, download the complete version of this article (containing all figures) from

http://spider.ipac.caltech.edu/staff/swolf/homepage/public/preprints/mfe.ps.gz

Fig. 2.— Histograms showing the distribution of the degree of polarization around the Bok globules B 335, CB 230, and CB 244.

and 5.1%. The corresponding 1σ dispersions are 3.7%, 4.1%, and 3.6%. These values are similar to those published in Paper I for the Bok globules CB 26, CB 54, and CG 30 (for polarization measurements in larger molecular clouds see Dowell 1997, Novak et al. 1997, Hildebrand 1996, Hildebrand et al. 1990, 1993, Morris et al. 1992, and Gonatas et al. 1990).

4.2. Magnetic fields

An estimate of the magnetic field strength (in units of G) can be derived from the polarization maps as follows (see Chandrasekhar & Fermi 1953)

$$B = |\vec{B}| = \sqrt{\frac{4\pi}{3}} \rho_{\text{Gas}} \cdot \frac{v_{\text{turb}}}{\sigma_{\bar{\gamma}}} .$$
(1)

Here, ρ_{Gas} is the gas density (in units of g cm⁻³), v_{turb} the rms turbulence velocity (in units of cm s⁻¹), and $\sigma_{\bar{\gamma}}$ the standard deviation to the mean orientation angle $\bar{\gamma}$ of the polarization vectors (in units of radians). Hereby, it is assumed that the magnetic field is frozen in the cloud material. For a detailed discussion of the applicability of this equation we refer to Paper I (§5.3).

Since the gas density ρ_{Gas} obviously strongly increases towards the center of each core, the magnetic field strength should be derived as a function of the radial distance from the density center. However, the small number of polarization vectors fulfilling the selection criteria discussed in §3 (see also Tab. 3) does not allow us to perform a statistical analysis on individual subsamples of polarization data points. Therefore, we decided to base our magnetic field estimates on the mean density from which the 850 μ m emission at a certain projected distance from the emission center arises. To ensure that the density value represents the region from which $\bar{\sigma}_{\gamma}$ was calculated, we used the mean distance of all considered polarization vectors from the center. These angular distances are B 335: 16.6", CB 230: 21.9", and CB 244 (SE core): 13.1".

We calculate the hydrogen number density profiles by using a ray-tracing code to fit spherically symmetric source models with an outer power-law density gradient to the observed, circularly averaged intensity maps. The model maps were convolved with the observed beam shape and chopping was accounted for. The mean dust temperature in the envelopes was determined by the $450/850 \,\mu$ m surface brightness ratio under the assumption that the dust opacity index $\beta = -1.8$ and $\kappa_{dust}(1.3 \,\mathrm{mm}) = 0.5 \,\mathrm{cm^2 g^{-1}}$. Dust temperatures in the range 10 to 14 K with an unresolved warmer core were derived, except for CB 26 and CB 54, which have higher temperatures and a global radial temperature gradient. Details of the models will be given in a forthcoming paper (Launhardt et al. in prep.). The derived

Object	$M_{ m H}^{ m env}$ [${ m M}_{\odot}$]	$\langle n_{\rm H} \rangle$ $[{\rm cm}^{-3}]$	$ ho_{ m Gas} \ [m gcm^{-3}]$	$v_{ m turb}$ $[m kms^{-1}]$	$N_{\rm vec}$	$\bar{\gamma}$ [°]	$\sigma_{ar{\gamma}}$ [°]	B $[\mu G]$
B 335	5	$3.8E{+}6$	8.6E-18	$0.14{\pm}0.02^{\rm a}$	20	-87.0	$35.8^{+14.6}_{-9.1}$	134_{-39}^{+46}
$\operatorname{CB}230$	7	$1.6E{+}6$	3.6E-18	$0.29 {\pm} 0.04^{\rm b}$	33	23.5	$29.8^{+8.8}_{-6.1}$	218^{+56}_{-50}
CB244 (SE core)	1.5	$3.5E{+}6$	8.0E-18	$\approx 0.29^{\circ}$	12	68.3	$33.1^{+19.2}_{-10.4}$	257^{+111}_{-91}
${ m CB}26^{ m e}$	0.27	$3.8E{+}5$	8.6E-19	$0.25^{\rm d}$	7	25.3	$18.9^{+16.7}_{-7.3}$	144_{-68}^{+91}
${ m CB}54^{ m e}$	100	$1.5E{+}5$	3.4E-19	$0.65^{\rm c}$	41	-68.0	$42.7^{+11.1}_{-8.0}$	104^{+24}_{-21}
$DC253\text{-}1.6^{\rm e,f}$	9	$2.2E{+}6$	5.0E-18	$0.25^{\rm d}$	49	14.4	$38.2^{+8.9}_{-6.6}$	172^{+36}_{-33}

Table 3. Masses, gas densities, polarization, and magnetic field strengths of the envelopes.

 $^{(a)}$ Frerking et al. 1987.

 $^{(b)}$ Wang et al. 1995; Launhardt et al. 1996.

 $^{(c)}$ Wang et al. 1995

 $^{(d)}No$ direct value available. rms turbulence velocity of a large sample of nearby star-forming Bok globules derived from C¹⁸O (J=2-1).

^(e)Re-derived mean density $\langle n_{\rm H} \rangle$ and corrected value for the magnetic field strength B.

 $^{(f)}{\rm The}$ magnetic field given for DC 253-1.6 in Tab. 2 of Paper I has to be corrected to $58^{+12}_{-11}\mu{\rm G}.$

envelope dust temperatures agree well with the kinetic gas temperatures derived by Cecchi-Pestellini et al. (2001) for a number of very similar southern Bok globules with protostellar cores. They also agree with the outer envelope temperature Evans et al. (2001) calculate for star-less globules which are heated interstellar radiation field only.

The dust emissivity is converted into hydrogen number density by using a standard hydrogen-to-dust mass ratio of 100. Details of the model will be given in a forthcoming paper (Launhardt et al. in prep.). To account for helium and heavy elements, we derive the total gas density ρ_{Gas} by

$$\rho_{\rm Gas} = 1.36 \cdot n_{\rm H} \cdot M_{\rm H},\tag{2}$$

where $M_{\rm H} = 1.00797 \,\mathrm{mu}$ is the mass of a hydrogen atom. The corresponding densities are listed in Tab. 3.

The next quantity to be derived from the polarization map in order to achieve an estimate of the magnetic field strength is the standard deviation of the orientation angle $\sigma_{\bar{\gamma}}$. The histograms of the orientation angle and the resulting standard deviations are shown in Fig. 3 and compiled in Tab. 3. Using CB 230 as an example, Fig. 4 also illustrates that a clear convergence towards a constant value of both quantities could be achieved on the basis of 18 complete polarization measurement cycles ("exposures"). For comparison, 27/15 exposures have been obtained for the globules B 335 and CB 244, respectively.

The error estimates for the value of the standard deviation of the mean orientation angle $\sigma_{\bar{\gamma}}$ is based on a χ^2 test assuming a standard Gaussian distribution of the orientations of the polarization vectors. The error intervals given in Tab. 3 are based on confidence intervals for $\sigma_{\bar{\gamma}}$. The probability for the real (unknown) $\sigma_{\bar{\gamma},\text{real}}$ to be included in this interval amounts to 95%. Based on this error estimate for $\sigma_{\bar{\gamma}}$, we give error intervals for the magnetic field strength B.

The magnetic fields – determined by the application of Equation 1 – are $B_{B335} \approx 130 \,\mu\text{G}$, $B_{CB230} \approx 220 \,\mu\text{G}$, and $B_{CB244} \approx 260 \,\mu\text{G}$. According to the investigations of theoretical models of polarized dust emission from protostellar cores by Padoan et al. (2001), these values might

Please, download the complete version of this article (containing all figures) from

http://spider.ipac.caltech.edu/staff/swolf/homepage/public/preprints/mfe.ps.gz

Fig. 3.— Histograms showing the distribution of position angles around B 335, CB 230, and CB 244. Only data points in which the 850 μ m flux exceeds 5 times the standard deviation and $P_1/\sigma(P_1) > 3$ have been considered.

have to be corrected by a factor of $f \approx 0.4$ in order to provide a better estimate of the average magnetic field strength in the cores.

In Paper I, we used volume-averaged densities, which are by a factor of about 3 (CB 54), 4 (CB 26), and 9 (DC 253-1.6) lower than those derived with our method applied here. For the sake of consistency and comparability, we re-derive densities and magnetic field strengths for these three sources and give the corrected values in Tab. 3. The magnetic field strengths in all six considered Bok globules are therefore very similar, amounting to ≈ 0.1 -0.3 mG. These magnetic field strengths are in the range of those values found in molecular clouds, pre-protostellar cores, and other star-forming regions (see, e.g., Matthews & Wilson 2002, Levin et al. 2001, Davis et al. 2000, Crutcher 1999, Glenn et al. 1999, Itoh et al. 1999, Minchin & Murray 1994, Chrysostomou et al. 1994, Bhatt & Jain 1992).

4.3. P_1 vs. I behavior

Similarly to previous polarization measurements in other star-forming cores (see, e.g., Matthews & Wilson 2002; Houde et al. 2002; Minchin et al. 1996; Glenn et al. 1999; see also Paper I), the degree of polarization was found to decrease towards regions of increasing intensity (see Fig. 5). This behaviour can be explained by either (i) an increase of the density in the brighter cores, resulting in an increased collisional disalignment rate of the grains towards the centers of the cores, (ii) grain growth in the denser regions resulting in unpolarized re-emission by the dust (Weintraub et al. 2000), or (iii) the fact that the field structure associated with the core collapse may be still unresolved in our polarization maps (see, e.g., Shu et al. 1987).

As outlined in Paper I, the decrease of the polarization towards increasing intensity can be approximately described by

$$P_1 = a_0 + a_1 \left(\frac{I}{\max(I)}\right)^{a_2},\tag{3}$$

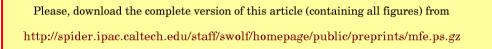


Fig. 4.— Top: Mean orientation angle $\bar{\gamma}$ of the polarization vectors as a function of the number of combined maps in the case of CB 230. The error bars mark the range $\bar{\gamma} \pm \sigma_{\bar{\gamma}}$. Bottom: Standard deviation to the orientation angle of the net polarization as a function of the number of combined maps in the case of CB 230.

Under the assumption that the physical properties of the dust grains are similar in the three Bok globules considered in this paper as well as in the Bok globules CG 30, CB 26, and CB 54 investigated in Paper I, the data points (162 in total) can be combined in order to derive a significantly better functional relationship between the intensity and polarization (and therefore the magnetic field strength than we could give in Paper I). To combine the data, the six separate intensity distributions have been normalized according to Eq. 3. We find the following parameters: $a_0 = -1.70$, $a_1 = 3.96$, $a_2 = -0.43$ for the best fit of Eq. 3 to the total data set (see Fig. 6). In fact, the average fit values for the entire sample are very similar to those found for CB 54 and DC 253-1.6 (see Paper I).

We remark that Eq. 3 represents an ad-hoc assumption about the relation between the polarization degree $P_{\rm I}$ and the corresponding intensity I, introduced to allow a first-order quantitative comparison of this relation for different Bok globules. A similar dependency $P_{\rm I}(I)$ was also found for other Bok globules and star-forming regions (Matthews & Wilson 2002; Houde et al. 2002; Minchin et al. 1996; Glenn et al. 1999; see also Paper I). A first qualitative confirmation of this observationally found non-linear dependency was provided by Padoan et al. (2001) on the basis of MHD simulations assuming no alignment of grains in regions with $A_{\rm V} > 3$ mag. A dependency in the form $P(n(\vec{r}), v_{\rm turb}(\vec{r}))$ is in fact expected if the decrease of the polarization degree is due to an increased disalignment rate of the dust grains in regions of high density and turbulence velocity.

Please, download the complete version of this article (containing all figures) from http://spider.ipac.caltech.edu/staff/swolf/homepage/public/preprints/mfe.ps.gz

Fig. 5.— Scatter diagrams showing the distribution of P_1 vs. intensity I across the Bok globules B 335, CB 230, and CB 240. Only data in which the 850 μ m flux exceeds 5 times the standard deviation, and $P_1/\sigma(P_1) > 3$ have been considered. Fits to the data sets of the data described by functions of the form $P_1 = a_0 + a_1(I/\max(I))^{a_2}$ are superposed on the data points (see §4.3).

4.4. Correlation between the magnetic field structure and the morphology of the Bok globules

All three globules (B 335, CB 230, and CB 244) contain Class 0 protostellar cores and drive collimated bipolar molecular outflows (Chandler & Sargent 1993, Yun & Clemens 1994, Launhardt 2001). Our polarization maps reveal alignment of polarization vectors and therefore the magnetic field with the outflow direction (most prominent in the case of B 335). Thus, the question arises whether the outflow direction is somehow related to the magnetic field structure given by the polarization maps. Since for two of our previously investigated globules (CB 26 and CB 54, see Paper I) we also know the outflow direction, we include these sources in our discussion here. The double core in DC 253-1.6 drives two nearly perpendicular outflows and is, therefore, not considered here. In discussing the relative orientation and relation between the magnetic field and the outflow one has to consider that only one component of the spatial orientation of the outflow $(v \sin i)$ is known from velocity measurements and the polarization vectors only allow to trace the projection of the magnetic field on the plane of the sky. In our analysis we assume that the magnetic field is oriented perpendicular to the measured polarization pattern. This widely applied concept is based on the finding that irrespective of the alignment mechanism, charged interstellar grains would have a substantial magnetic moment, leading to a rapid precession of the grain angular momentum Jaround the magnetic field direction \vec{B} which implies a net alignment of the grains with the magnetic field (see, e.g., Draine & Weingartner 1997).

The $850 \,\mu\text{m}$ polarization maps overlayed with the blue- and redshifted outflow velocity contour lines of B 335, CB 230, CB 244, CB 26, and CB 54 are shown in Fig. 7-9. Since the outflows have been mapped using different radio telescopes, the spatial resolution varies strongly but the main features, i.e., the orientation with respect to the aligned polarization vectors can be clearly seen:

B 335 (Fig. 7, left): Nearly *parallel* alignment of the polarization vectors (and therefore the mean polarization) with the outflow axis. The globule is clearly elongated in North-South direction (see Fig. 1), and therefore oriented perpendicular to the polarization pattern and parallel to the magnetic field. Based on investigations of axis ratios of large samples of Bok globules, Myers et al. (1991) and Ryden (1996) found that oblate cores would be inconsistent with the observed axis ratios to a high confidence level. Thus, we assume that B 335 is a prolate globule rather than an oblate one seen edge-on. The orientation of the magnetic field parallel to the symmetry axis of the globule fits into the scenario described by Fiege & Pudritz (2000a; see also Fiege & Pudritz 2000c), assuming the case $B_z/B_{\Phi} > 0.37$, where B_z and B_{Φ} are, respectively, the ploidal and toroidal magnetic field components at the outer surface of the globule core. Their theoretical investigations of molecular cloud cores that

Please, download the complete version of this article (containing all figures) from http://spider.ipac.caltech.edu/staff/swolf/homepage/public/preprints/mfe.ps.gz

Fig. 6.— Left: Scatter diagram showing the distribution of P_1 vs. intensity I across the Bok globules B 335, CG 30, CB 54, CB 230, CB 240, and CB 244 (SE core). The data for the Bok globules CG 30, CB 26, and CB 54 have been taken from Paper I. The solid line represents the best fit of the function given in Eq. 3. Right: Corresponding distribution of the polarization degree as a function of the hydrogen density (see §4.3). If the measurements for CB 54 (symbolized by triangles) were excluded from this plot, a nearly linear dependency between the polarization degree and gas density is reaveled for densities $\log_{10} n_{\rm H} < 8$. What distinguishes CB 54 from the other objects is the fact that it most likely contains several unresolved sources (see Paper I for a detailed description of this source).

Please, download the complete version of this article (containing all figures) from

http://spider.ipac.caltech.edu/staff/swolf/homepage/public/preprints/mfe.ps.gz

Fig. 7.— SCUBA intensity map $(850\,\mu{\rm m})$ of the Bok globules B 335 and CB 230 with overlayed

- 1. Iso-intensity contour lines in the case of CB 230 (thin dotted lines; $850 \,\mu\text{m}$; contour levels: 0.15%, 0.30%, 0.45%, 0.60%, 0.75%, and 0.90% of the maximum intensity I_{max} . For reason of clarity, iso-intensity contour lines corresponding to the $850 \,\mu\text{m}$ SCUBA intensity map are not shown in the case of B 335 see Fig. 1(top) for this information.),
- 2. Polarization pattern (850 μ m, see Fig. 1 for details), and
- 3. ¹³CO(1-0) spectral channel maps obtained with OVRO. **B** 335: The white/grey contour lines represent the spatially well-separated blue/red shifted western/eastern outflow lobe. The contours are spaced at 2σ intervals of 200 mJy beam⁻¹ (from Chandler & Sargent 1993; beam width: 2.9"×2.9"). **CB** 230: The solid/dashed contour lines represent the spatially well-separated blue-shifted/red-shifted outflow lobe (beam width: 4"). Blue lobe: $v_{\rm LSR} = 1.6...2.8 \,\rm km \, s^{-1}$ (solid contours), red lobe: $v_{\rm LSR} = 3.0...4.2 \,\rm km \, s^{-1}$ (dashed contours). The step width amounts to 0.3 km s⁻¹ for both lobes (from Launhardt 2001). See also Yun & Clemens (1994, Fig. 27) for a large-scale outflow map (6' × 6').

originate from filamentary clouds which are threaded by helical magnetic fields show that the radial pinch of the toroidal field component helps to squeeze cores radially into a prolate shape while helping to support the gas along the axis of symmetry. In the context of star formation inside Bok globules it is of interest that the Bonnort-Ebert critical mass is reduced by about 20% by the toroidal field. Assuming that the predicted submillimeter polarization patterns for filamentary clouds are valid for elongated Bok globules as well, we can not completely confirm the predictions by Fiege & Pudritz 2000b (see Fig. 1 in their work for different magnetic field/polarization pattern scenarios). Based on model simulations, these authors find depolarization along the axis of the filaments. While we find depolarization towards the center of the Bok globules as well (see §4.3 for a detailed analysis of this effect), the radial dependence of the polarization degree in the outer regions of the Bok globules does not agree with the theoretical findings for filamentary structures.

CB 230 (Fig. 7, right): Alignment of the mean polarization almost *parallel* to the outflow axis. The decrease of the linear polarization towards the bright globule core is slightly stronger towards the red-shifted side of the lobe. The globule is slightly elongated in E-W direction and therefore, like in the case of B 335 (under the assumption of a spheroidal shape) elongated perpendicular to the polarization pattern and parallel to the magnetic field direction, respectively.

CB 244 (Fig. 8, left): Apparent alignment of the polarization vectors between the dominant SE core and the NW source parallel to the density enhancement between both sources. If higher resolved polarization maps with a sufficient, statistically larger sample of polarization vectors in this region will confirm this finding, it would support the hypothesis of matter infall along magnetic field lines during the initial stage of molecular cloud collapse.

Close to the main (SE) source, however, the orientation of the polarization vectors seems to change slightly towards a preferential direction parallel of the outflow axis and therefore perpendicular to the orientation of the dust/gas "bridge" between both sources. One has to consider that the orientations of the small number of polarization vectors in the SE core show a large scatter. A higher resolved polarization map would be required in order to confirm the change of the polarization/magnetic field orientation towards the SE core. This would also help to decide whether the magnetic field is aligned with the outflow (and therefore oriented in the same direction as in the region of the density enhancement between both sources) or if the outflow and/or other processes related to the ongoing star formation process in the SE core cause(d) a change of the magnetic field orientation.

The core of CB 244 is slightly elongated in E-W direction and therefore - in contrast to B 335 and CB 230 - more aligned with the mean polarization direction than perpendicular to it. However, if the change of the polarization within the SE core is real, a similar scenario

Please, download the complete version of this article (containing all figures) from

http://spider.ipac.caltech.edu/staff/swolf/homepage/public/preprints/mfe.ps.gz

Fig. 8.— SCUBA intensity map $(850\,\mu{\rm m})$ of the Bok globule CB 244 and CB 54 with overlayed

- 1. Iso-intensity contour lines (thin solid lines; $850 \,\mu\text{m}$; contour levels: 0.15%, 0.30%, 0.45%, 0.60%, 0.75%, and 0.90% of the maximum intensity I_{max}),
- 2. Polarization pattern (850 μ m, see Fig. 1 for details), and
- 3. ¹²*CO J=1-0 spectral line map* (from Yun & Clemens 1994). The broad solid/dashed contour lines represent the blue/red integrated line wing emission. These maps were obtained with a 15 beam receiver with an antenna had beam width of 48" (FWHM; for comparison: SCUBA FWHM amounts to 14.7" at 850 μ m). **CB 244**: Blue/red-shifted outflow contour lines begin with 0.5 K km s⁻¹/0.6 K km s⁻¹ and are stepped by 0.15 K km s⁻¹/0.2 K km s⁻¹. **CB 54**: Blue/red-shifted outflow contour lines begin with 1.7 K km s⁻¹/0.45 K km s⁻¹ and are stepped by 0.3 K km s⁻¹/0.15 K km s⁻¹.

as described for the other two globules is expected.

CB 54 (Fig. 8, right): This is a large Bok globule associated with the molecular cloud BBW 4 in a distance of about 1.1 kpc (Brand & Blitz 1993). In contrast to B 335 and CB 230, the mean polarization direction is found to be almost *perpendicular* to the outflow axis. However, one has to consider that (a) the polarization pattern shows a large scatter of the orientation of the individual polarization vectors and (b) the much larger distance of the object (compared to the other investigated globules) does not allow to resolve structures of comparable size, i.e., the orientation of the magnetic field on the scale as measured in the case of the other globules is not known. The polarization measurements trace a magnetic field structure which is extended much more further out into the surrounding interstellar space and may therefore be much more representative for the interstellar magnetic field structure in this region than for the local magnetic field structure of CB 54.

This globule is slightly elongated in S-E/N-W direction, almost parallel to the direction of the mean polarization, which is in contrast to the Bok globules B 335 and CB 230. However, due to the much higher spatial distance of CB 54, we can not rule out that this globule consists of several substructures (smaller globule cores) which are not resolved in our intensity maps. This possibility is supported by the finding that a small young near-infrared stellar cluster which was probably born in CB 54 is projected against the the dense core of this globule (Yun 1996, Launhardt 1996).

CB 26 (Fig. 9): This small, slightly cometary-shaped Bok globule at a distance of about 140 pc (Launhardt et al. in prep.) contains a small bipolar near-infrared nebula which is associated with strong submillimeter/millimeter continuum emission. The star responsible for the reflection nebula (see Fig. 9, right frame) is deeply embedded and not seen even at 2.2 μ m. No large-scale outflow was observed, but the edge-on circumstellar disk found by Launhardt & Sargent (2001) as well as the bipolar structure perpendicular to the disk midplane suggest either the existence of an outflow in the plane of the sky (for which the velocity field could not be traced) or, at least, a very weak outflow. The orientation of the mean polarization differs by about 35° from the orientation of the disk. As in the case of CB 54 we find the mean polarization direction (N-E/S-W) to be slightly aligned perpendicular to the outflow direction. The small number of polarization vectors does not allow to trace the expected randomly oriented polarization vectors in the inner part of the globule.

The comparison with the results of an analytic investigation of the final states for a quasimagnetostatic phase of the evolution of molecular cloud cores by ambipolar diffusion (based on a magnetized singular isothermal toroid model) by Li & Shu (1996) describes the scenario probably found in the case of CB 26. As Fig. 1 in their publication shows, an hourglassshaped magnetic field structure is oriented perpendicular to an already formed (proto)circumstellar disk. Taking into account the low resolution of our polarization maps, this magnetic field pattern translates into an almost parallel polarization pattern with an orientation parallel to the disk and perpendicular to the outflow, respectively. Another prediction of their model is that at this stage the magnetic field structure in the inner core would be very complex due to inflowing gas colliding with the expanding outflows. In agreement with our observations, the polarization vectors would be much more randomly oriented in the core. At this point we would like to remined the reader that this discussion is based on a statistically very small number of polarization vectors only. A higher resolved polarization map is required to confirm the conclusions drawn above.

We want to conclude the most interesting findings concerning the connections between the magnetic field topology and Bok globule morphology of the globule cores (see also Tab. 4):

- 1. The globules B 335 and CB 230 show a slightly elongated shape which we assume in the following to be the projection of a prolate spheroid on the plane of the sky (in agreement with the theoretical and observational findings by Fiege & Pudritz 2000a/c, Myers et al. 1991, and Ryden 1996 as discussed above). We exclude the CB 26 and CB 54 cores, which are also elongated, from this discussion. In contrast to the other sources, CB 26 is a remnant envelope around a young protostellar disk and CB 54 is a large and massive globule which may contain multiple unresolved cores.
- 2. We find the direction of
 - (a) The polarization vectors/magnetic field,
 - (b) The elongation of the Bok globules, and
 - (c) The orientation of the outflows (in the case of CB 26: potential outflow direction)

to be not independent (= arbitrarily oriented) but related to one another.

- 3. The direction of the outflows of B 335 and CB 230 is almost *perpendicular* to the orientation of the elongation direction of the globules, i.e., perpendicular to the potential projection of the symmetry axis on the plane of the sky.
- 4. In the case of B 335 and CB 230 the outflows are oriented almost *parallel* to the preferential direction of the linear polarization, i.e., perpendicular to the magnetic field (both as seen in projection on the plane of the sky).
- 5. In the case of CB 54 and CB 26 the outflows are oriented slightly *perpendicular* to the preferential direction of the linear polarization, i.e., parallel to the magnetic field.

Table 4. Outflow and Magnetic Field orientations.

	Mean Magnetic field direction [°]	Mean Outflow orientation [^o]	Angle between outflow and Magnetic field orientation
CB 26	$-65(\pm 19)$	$-29^{(a,e)}$	36
$\mathrm{CB}~54$	$22(\pm 43)$	$30^{(b)}$	8
CB 230	$-67(\pm 30)$	$0^{(b,c)}$	67
B 335	$3(\pm 36)$	$-80^{(d)}$	83
$\mathrm{CB}~244$	$-22(\pm 33)$	$45^{(b)}$	67

The error interval given in case of the magnetic field directions are equivalent to the standard deviation to the mean orientation angle of the polarization (see Tab. 3 this paper and Tab. 2 in Paper I).

 $^{(a)}$ Launhardt & Sargent (2001)

 $^{(b)}$ Yun & Clemens (1994)

 $^{(c)}$ Launhardt (2001)

 $^{(d)}$ Hirano et al. (1988)

 ${}^{(e)}\text{P.A.}(\text{disk}):~60^{\rm o}\pm5^{\rm o}$ (Launhardt & Sargent 2001)

However, due to the large scattering of polarization directions measured in CB 54 and the small number of polarization vectors and low spatial resolution in the case of CB 26, the statistical significance of these results is low. In the particular case of the globule CB 26, a spatially higher resolved polarization map would be required to confirm the apparent alignment between the direction of the potential outflow direction and the magnetic field.

We exclude CB 244 from this overview since we can hardly separate the magnetic field structure related to the density enhancement reaching from the main (SE) source to the secondary (NW) source from the magnetic field structure being dominant at the position of the main source alone.

We compared our polarization maps to those resulting from magneto-hydrodynamic (MHD) simulations of molecular clouds performed by Padoan et al. 2001 (Fig. 5; see also Heitsch et al. 2001, Fig. 5 for comparison). In agreement with many of these simulations our observations of B 335, CB 230, and CB 26 show large-scale alignment of the polarization vectors with smooth changes of the orientation also on large scale only. Similar to the simulated polarization pattern in Fig. 5d by Padoan et al. (2001), the change of the direction of the polarization vectors at the transition from the high-dense Bok globule towards the lower-dense gas/dust "bridge" between the two cores in CB 244 can be seen. Furthermore, our observations of B 335 and CB 230 show not only a decrease of the polarization degree (see §4.3 for a detailed analysis), but also that the orientation of the polarization vectors does not remarkably change towards the dense cores. This supports the hypothesis that despite the decrease of the grain alignment rate, the magnetic field structure in the cores of these objects is not seriously disturbed, and thus still representing the primordial field. In the case of CB 244 and CB 54 on the other hand, the orientation of the polarization vectors and therefore the structure of the magnetic field in the cores is chaotic and we assume that it can not longer be accounted for being representative for the primordial field. Thus, one might expect that CB 26 represents a more evolved protostellar systems than the globules B 335 and CB 230. However, the data available so far, in particular the low-resolution, low-sampled polarization map of CB 26, do not allow to place this assumption as a strong conclusion. A higher-resolved, better-sampled polarization map of CB 26 would help to confirm this hypothesis.

Spatially higher resolved polarization maps would simultaneously allow to test another theoretical prediction about the protostellar evolution based on which the different orientations of the magnetic field relative to the outflow direction of B 335 and CB 230 on the one hand and CB 26 on the other hand could be explained: Tomisaka (1998) showed on the basis of MHD simulations of collapse-driven outflows in molecular cores that the direction

of the magnetic field lines and the disk plane decreases from $60^{\circ}-70^{\circ}$ to $10^{\circ}-30^{\circ}$ during the evolution of the outflow (Fig. 2a,b in his publication). At least on the large scale, our observations are in agreement with this scenario: Since our polarization maps do not resolve structures with the size of a circumstellar disk, the magnetic field direction as derived from the polarization maps, would change from an orientation *parallel to the disk midplane* to an orientation *perpendicular to the disk midplane* during the evolution of the protostar and its outflow in particular.

5. Conclusions

Using the Submillimeter Common User Bolometer Array (SCUBA) at the JCMT we obtained 850 μ m polarization maps with a resolution of 9' × 9' of the Bok globules B 335, CB 230, and CB 244. We find polarization degrees equally distributed in the range $P_1 = 0 - 14\%$. Using the formalism by Chandrasekhar & Fermi (1953) we derive an estimate of the mean magnetic field strengths in these globules in the order of several hundred μ G. These values are slightly higher than those discussed in Paper I based on another sample of Bok globules (B=20-100 μ G) but are still comparable to typical magnetic field strengths found in molecular clouds, pre-protostellar cores, and other star-forming regions (see §4.2 for references). The magnetic fields derived here are higher because we based our calculations on a higher density closer to the globule centers for the magnetic field estimates (see §4.2).

We find a similar correlation between the polarization degree and the intensity and therefore the density of the emitting dust as measured in other star-forming cores (see §4.3 for references). We verify the non-linear relation between these quantities first stated in Paper I. However, the particular equation used to parameterize the decrease of the polarization with increasing intensity (Eq. 3) is a first-order approximation only (see §4.3, Fig. 6). MHD simulations show qualitatively similar results (Padoan et al. 2001) but a quantitative description of this phenomenon is still lacking. Here, different grain (dis)alignment processes in the centers of Bok globules, such as discussed in Paper I will have to be considered in much more detail in these simulations (see, e.g., Lazarian 1997 and Lazarian et al. 1997).

The main question we focussed on in this work is related to the search for correlations between the structure of the magnetic field and particular features of Bok globules. In addition to the globules B 335 and CB 230 we reconsider the globules CB 26 and CB 54 (from Paper I) as well. Because of the more complex structure of the Bok globule CB 244, this object is only partly considered in this investigation (see §4.4). Furthermore, CB 54 may represent an unresolved ensemble of Bok globules. As common criteria to characterize the main spatial structure of the Bok globules we take into account (a) the orientation of the slightly elongated core (in case of B 335 and CB 230) and (b) the orientiation of the outflow (or the expected outflow in the case of CB 26). Based on the theoretical studies by Fiege & Pudritz (2000a,c) and observational constraints by Myers et al. (1991) and Ryden (1996) we assume that all these 4 globules have a prolate shape rather than an oblate one.

We find that the outflows are oriented almost perpendicular to the symmetry axis of the globule cores in case of the globules B 335 and CB 230. The elongations found in case of CB 54 and CB 26 have a similar orientation, but the lower (absolute) spatial resolution of CB 54 and the possible influence of a neighboring object of CB 26 may have changed the intrinsic globule shape. The magnetic field, however, is aligned with the symmetry axis of the prolate cores in the case of the Bok globules B 335 and CB 230, while it is slightly aligned with the outflow axis in the case of the Bok globules CB 26 and CB 54. Since the symmetry axis of the core is expected to be aligned with the magnetic field in order to explain the observed high abundance of prolate Bok globules, we assume that the magnetic field structure found in the case of the globules B 335 and CB 230 represents the primordial magnetic field which is nearly undisturbed even in the innermost regions of these globule cores. The polarization decreases towards the centers of these cores but the orientation of the linear polarization and therefore, prependicular to it, the orientation of the magnetic field, is the same as on larger scales. The polarization maps of these two objects allow to resolve structures with diameters of about 2×10^3 AU (B 335) and 4×10^3 AU (CB 230). If the magnetic field structure in the circum-(proto)stellar environment differs strongly from the large-scale magnetic field direction, these pertubations must occur on much smaller scales than given by the resolution of the polarization maps in order to allow the net polarization to be aligned with the large-scale magnetic field structure. Furthermore, we cannot exclude the case that the magnetic field structure is very complex on scales much smaller than the resolution of the polarization maps. Then, the net polarization arising from the inner core is likely to be negligible and all we measure is the small contribution of polarized light from the foreground material.

Following the results of hydrodynamic simulations by Tomisaka (1998) and theoretical investigations of the protostellar evolution by Li & Shu (1996), the orientation of the magnetic field relative to the outflow direction is not constant but changes during the evolution of the outflow/disk. Taking into account the comparably low resolution of our polarization maps, this change would result in

- 1. A polarization pattern which is oriented parallel to the outflow (*mean magnetic field* perpendicular to the outflow) at the beginning of the outflow changing to
- 2. A negligible polarization in the range of the core due to polarization cancelation (averaging) effects at some point during the evolution of the outflow, and finally to

3. A polarization pattern which is oriented perpendicular to the outflow (*mean magnetic field parallel to the outflow*) at the late stage of the evolution of the outflow.

Within this frame, our results for the Bok globules B 335 and CB 230 are consistent with an evolutionary stage somewhere between step 1 and 2. Furthermore, the different relative orientation of the magnetic field relative to the outflow direction / circumstellar disk orientation in case of CB 26 suggests that this object already reached evolutionary stage 3. However, a better sampled, higher resolved (sub)millimeter polarization map is required in order to confirm this assumption.

We conclude that our observations suggest an evolution of the magnetic field of protostellar systems embedded in Bok globules. Our findings do agree with theoretically predicted scenarios at this very early stage of stellar evolution, both in respect of the alignment of the magnetic field with the elongated globule as well as with the correlation between the magnetic field direction relative to the outflow direction.

REFERENCES

- Alves, J.F., Yun, J.L. 1995, ApJ, 438, L107
- André, P., Ward-Thomson, D., Barsony, M. 1993, ApJ, 406, 122
- Barnard, E.E. 1927, A Photographic Atlas of Selected Regions of the Milky Way II. Charts and Tables (Pub. 247) (Washington, DC: Carnegie Inst. Washington)
- Berry, D.S., Gledhill, T.M. 1999, Starlink UserNote 223
- Bhatt, H.C., Jain, S.K. 1992, MNRAS, 257, 57
- Bok, B.J. 1977, PASP, 89, 597
- Brand, J., Blitz, L. 1993, A&A, 275, 67
- Cabrit, S., Goldsmith, P. F., Snell, R. L. 1988, ApJ, 334, 196
- Cecchi-Pestellini, C., Casu, S., Scappini, F. 2001, MNRAS, 326, 1255
- Clemens, D.P., Barvainis, R. 1988, ApJS, 68, 257
- Clemens, D.P., Yun, J.L., Heyer, M.H. 1991, ApJS, 75, 877

- Chandler, C. J., Gear, W. K., Sandell, G., Hayashi, S., Duncan, W. D., Griffin, M. J., Hazella, S. 1990, MNRAS, 243, 330
- Chandler, C.J., Sargent, A.I. 1993, ApJ, 414, L29
- Choi, M., Evans, N. J., Gregersen, E. M., Wang, Y. 1995, ApJ, 448, 742
- Chrysostomou, A., Hough, J.M., Burton, M.G., Tamura M. 1994, MNRAS, 268, 325
- Crutcher, R.M. 1999, ApJ, 520, 706
- Davis, C.J., Chysostomou, A., Matthews, H.E., Jenness, T., Ray, T.P. 2000, ApJ, 530, L115
- Dowell, C.D. 1997, ApJ, 487, 237
- Draine, B.T., Weingartner, J.C. 1997, ApJ, 480, 633
- Evans, N.J., II, Rawlings, J.M.C., Shirley, Y.L., Mundy, L.G. 2001, ApJ, 557, 193
- Fiege, J.D., Pudritz, R.E. 2000a, ApJ, 534, 291
- Fiege, J.D., Pudritz, R.E. 2000b, ApJ, 544, 830
- Fiege, J.D., Pudritz, R.E. 2000c, MNRAS, 311, 105
- Frerking, M. A., Langer, W. D., Wilson, R. W. 1987, ApJ, 313, 320
- Glenn, J., Walker, C.K., Young, E.T. 1999, ApJ, 511, 812
- Gonatas, D.P., Engargiola, G.A. Hildebrand, R.H., Platt, S.R., Wu, X. D., et al. 1990, ApJ, 357, 132
- Greaves, J.S., Holland, W.S., Minchin, N.R., Murray, A.G., Stevens, J.A. 1999, A&A, 334, 668
- Greaves, J.S., Jennes, T., Chrysostomou, A.C., Holland, W.S., Berry, D.S. 2000, in ASP Conf. Ser. 217, Imaging at Radio through Submillimeter Wavelengths, ed. J.G. Mangum & S.J.E. Radford (San Francisco: ASP), p. 150
- Heitsch, F., Zweibel, E.G., Mac Low, M.M., Li, Pakshing, Norman, M.L. 2001, ApJ, 561, 800
- Henning, Th., Launhardt, R. 1998, A&A, 338, 223
- Henning, Th., Wolf, S., Launhardt, R., Waters, R. 2001, ApJ, 561, 871 (Paper I)

- Hildebrand R.H. 1996, in ASP Conf. Ser. 97, Polarimetry of the Interstellar Medium, ed. W.G. Roberge & D.C.B. Whittet (San Francisco: ASP), 254
- Hildebrand, R.H., Davidson, J.A., Dotson, J., Figer, D.F., Novak, G., Platt, S.R., Tao, L. 1993, ApJ, 417, 565
- Hildebrand, R.H., Gonatas, D.P., Platt, S.R., Wu, X.D., Davidson, J.A., Werner, M.W., Novak, G., Morris, M. 1990, ApJ, 362, 114
- Hirano, N., Kameya, O., Nakayama, M., Takakubo, K. 1988, ApJ, 327, L69
- Holland, W.S., Robson, E.I., Gear, W.K., Cunningham, C.R., Lightfoot, J.F., et al. 1999, MNRAS, 303, 659
- Houde, M., Bastien, P., Dotson, J.L., Dowell, C.D., Hildebrand, R.H., et al. 2002, ApJ, 569, 803
- Huard, T.L., Sandell, G., Weintraub, D.A. 1999, ApJ, 526, 833
- Itoh, Y., Chrysostomou, A., Burton, M., Hough, J.H., Tamura, M. 1999, MNRAS, 304, 406
- Jenness, T., Lightfoot, J.F. 1998, in ASP Conf. Ser. 145, Astronomical Data Analysis Software and Systems VII, ed. R. Albrecht, R.N. Hook, & H.A. Bushouse, (San Francisco: ASP), 216
- Jenness, T., Lightfoot, J.F., Holland, W.S. 1998, Proc. SPIE, 3357, 548
- Keene, J., Davidson, J. A., Harper, D. A., Hildebrand, R. H., Jaffe, D. T., Loewenstein, R. F., Low, F. J., Pernic, R. 1983, ApJ, 274, L43
- Khanzadyan, T., Smith, M.D., Gredel, R., Stanke, T., Davis, C.J. 2002, ApJ, 383, 502
- Kim, H.G., Hong, S.S. 2002, ApJ, 567, 376
- Kun, M. 1998, ApJS, 115, 59
- Launhardt, R. 1996, Ph.D. Thesis, Univ. of Jena
- Launhardt, R. 2001, In "Birth and Evolution of Binary Stars", Reipurth B. & Zinnecker H. (eds.), Proceedings of IAU Symposium No. 200, p. 117
- Launhardt, R., Evans, N.J., Wang, Y., Clemens, D.P., Henning, Th., Yun, J.L. 1998, ApJSS, 119, 59
- Launhardt, R., Henning, Th. 1997, A&A, 326, 329 (LH97)

- Launhardt, R., Sargent, A. 2001, ApJ 562, L173
- Launhardt R., Ward-Thompson D., Henning Th. 1997, MNRAS, 288, L45
- Lazarian, A. 1997, MNRAS, 288, 609
- Lazarian, A., Goodman, A.A., Myers, P.C. 1997, ApJ, 490, 273
- Leung, C.M. 1985, Physical conditions in isolated dark globules. In: Black D.C., Matthews M.S. (eds.), Protostars and Planets II, University of Arizona Press, p. 104
- Levin, S.M., Langer, W.D., Velusamy, T., Kuiper, T.B.H. 2001, ApJ, 555, 850
- Li, Z.-Y., Shu, F.H. 1996, ApJ, 472, 211
- Lynds, B.T. 1962, ApJS, 7, 1
- Matthews, B.C., Wilson, C.D. 2002, ApJ, 574, 822
- Myers, P.C., Fuller, G.A., Goodman, A.A., Benson, P.J. 1991, ApJ, 376, 561
- Minchin, N.R., Bonifaćio, V.H.R., Murray, A.G. 1996, A&A, 315, L5
- Minchin, N.R., Murray, A.G. 1994, A&A, 286, 579
- Moreira, M.C., Yun, J.L. 1995, ApJ, 454, 850
- Morris, M., Davidson, J.A., Werner, M., Dotson, J. Figer, D.F., Hildebrand, R., Novak, G., Platt, S.R. 1992, ApJ 399, L63
- Murray, A.G., Nartallo, R., Haynes, C.V., Gannaway, F., Ade, P.A.R. 1997, in Proc. ESA Symp., The Far Infrared and Submillimeter Universe, ed. A. Wilson (Noordwijk: ESA), 405
- Myers, P. C., Evans, N. J., Ohashi, N. 2000, in Protostars and Planets IV, ed. V. Mannings, A.P. Boss, & S.S. Russell (Tucson: Univ. Arizona Press), 217
- Myers, P.C., Goodman, A.A., Gusten, R., Heiles, C. 1995, ApJ, 442, 177
- Novak, G., Dotson, J.L., Dowell, C.D., Goldsmith, P.F., Hildebrand, R.H., Platt, S.R., Schleuning, D.A. 1997, ApJ, 487, 320
- Padoan, P., Goodman, A., Draine, B., Juvela, M., Nordlund, Å., Rögnvaldsson, O. 2001, ApJ, 559, 1005

- Ryden, B.S. 1996, ApJ, 471, 822
- Shu, F. H. 1977, ApJ, 214, 488
- Shu, F., Adams, F., Lizano, S. 1987, ARA&A, 25, 23
- Tomisaka, K. 1998, ApJ, 502, L163
- Tomita, Y., Saito, T., Ohtani, H. 1979, PASJ, 31, 407
- Wang, Y., Evans, N.J.II, Zhou, S., Clemens, D.P. 1995, ApJ, 454, 217
- Weintraub, D.A., Goodman, A.A., Akeson, R.L. 2000, in Protostars and Planets IV, ed. V. Mannings, A.P. Boss, & S.S. Russell (Tucson: Univ. Arizona Press), 247
- Wilner, D. J., Myers, P. C., Mardones, D., Tafalla, M. 2000, ApJ, 544, L69
- Yun, J. L. 1996, AJ, 111, 930
- Yun, J.L., Clemens, D.P., McCaughrean, M., Rieke, M. 1993, ApJ, 408, L101
- Yun, J.L., Clemens, D.P. 1994a, ApJS, 92, 145
- Yun, J.L., Clemens, D.P. 1994b, AJ, 108, 612
- Yun, J.L., Moreira, M.C., Torrelles, J.M., Alfonso, J.M., Santos, N.C. 1996, AJ, 111, 841
- Zhou, S., Evans, N. J., Kömpe, C., Walmsley, C. M. 1993, ApJ, 404, 232

The authors wish to acknowledge R. Tilanus for supporting the observations and data reduction. This research was supported by the DFG grant Ste 605/10 within the program "Physics of Star Formation", and by the travel grant He 1935/22-1 of the DFG. S.W. acknowledges support through the HST Grant GO 9160, and through the NASA grant NAG5-11645. JCMT is operated by the Joint Astronomical Centre on behalf of the UK Particle Physics and Astronomy Research Council. We wish to thank the anonymous Referee for helpful comments concering the discussion of the results.

This preprint was prepared with the AAS IATEX macros v5.0.

Please, download the complete version of this article (containing all figures) from

http://spider.ipac.caltech.edu/staff/swolf/homepage/public/preprints/mfe.ps.gz

Fig. 9.— Left: SCUBA intensity map $(850 \,\mu\text{m})$ of the Bok globule CB 26 with overlayed

- 1. Iso-intensity contour lines (thin dotted lines; $850 \,\mu\text{m}$; contour levels: 0.15%, 0.30%, 0.45%, 0.60%, 0.75%, and 0.90% of the maximum intensity I_{max}),
- 2. Polarization pattern (850 μ m; see Fig. 7 for details).

(from Paper I). Furthermore, the mean direction of the polarization $\bar{\gamma}$ is shown. The range of $\bar{\gamma} \pm \sigma_{\bar{\gamma}}$ is marked.

Right: Central part of the Bok globule CB 26 (from Launhardt & Sargent 2001). J - H color map of the bipolar near-infrared reflection nebula (black contour lines: K band emission). The white contour lines show the proto-planetary disk discovered by Launhardt & Sargent (2001; contour levels: 4, 11, 18, 25, and 32 mJy $\operatorname{arcsec}^{-2}$; obtained with OVRO at 1.3 mm - beam width: 0.58"×0.39").